Self-Aggregation of DNA Oligomers with XGG Trinucleotide Repeats: Kinetic and Atomic Force Microscopy Measurements

Feng Sha,* Rixiang Mu,# Don Henderson,# and Fu-Ming Chen*
*Department of Chemistry, Tennessee State University, Nashville, and #Chemical Physics Laboratory, Department of Physics, Fisk University, Nashville, Tennessee 37209-1561 USA

ABSTRACT Turbidity measurements via absorbance monitoring at 320 nm were employed to obtain autocatalytic-like kinetic profiles of K^+-induced aggregate formation of $d(XGG)_4$ and some related oligomers, where X = A, C, G, and T. At least 1 M KCl is needed to observe the turbidity-measurable aggregation at pH 8, and the relative propensity for aggregate formation is shown to follow the order $d(GGG)_4 > d(AGG)_4 \approx d(TGG)_4 \gg d(CGG)_4$. The presence of Mg^{2+} greatly facilitates and dramatically reduces the amount of K^+ required to initiate aggregation and significantly enhances the thermal stabilities of the aggregates. Replacement of K^+ by Na^+ fails to induce a similar phenomenon. The Ψ-type CD characteristics of aggregates are strongly dependent on the sequence and ionic conditions. Despite their ease of aggregate formation, oligomers with AGG trinucleotide repeats fail to exhibit Ψ-CD formation. The propensity for aggregation is greatly affected by the chain length, with oligomers of four repeats being most facile. Appending X base at the 3′ end of d(GGXGGXGGXGG) appears to provide a greater hindrance to aggregation than at the 5′ end. Atomic force microscopic images support some of these findings and reveal the morphologies of these aggregates. The presence of $MgCl_2$ in solutions appears to considerably elongate the K^+-induced aggregates.

INTRODUCTION

Structural properties of G-rich DNA are of current intense interest, as they may be intimately related to the telomeric functions. Telomeres are specialized DNA-protein structures at the termini of chromosomes that have been shown to be important for their stability and accurate replication (Lumdblad and Szostak, 1989; Sandell and Zakian, 1993; Blackburn, 1994). Telomeric DNAs consist of simple repetitive guanine-rich sequences, with the most common units consisting of three or four guanine nucleotides. It has been shown that these G-rich oligomers can form intermolecular or intramolecular G-quadruplexes, depending on the chain length and intervening non-G nucleotides, with strong dependence on the monovalent cations such as K^+ and Na^+ (Williamson, 1994). These tetraplexes are cyclic arrays of four hydrogen-bonded guanine bases in which each base acts as both donor and acceptor of two hydrogen bonds with other guanines, and the pairing between bases is of the Hoogsteen type. The interest in these structures has been further stimulated by their possible relevance to the recombinational events at the immunoglobulin switching regions (Sen and Gilbert, 1988). Effects of monovalent cations on the G-quadruplex structural formation of telomeric DNA sequences have been extensively studied in recent years. Evidence suggests that K^+ is much more effective in stabilizing G-quadruplex formation, possibly because of its optimal size. The ion is found to be sandwiched between two G-tetrads to form an octacoordinated complex with the carbonyl groups of guanines. It was also found that for contiguous guanine oligomers, the parallel strand orientation is thermodynamically more favorable than the antiparallel orientation in the G-quadruplex formation (Sen and Gilbert, 1988; Lu et al., 1993).

A rather interesting phenomenon, likely related to quadruplex structures, was uncovered earlier in our laboratory, in which molar K^+ induces chiral aggregate formation in $d(CGG)_4$ (Chen, 1995). The kinetics of this transformation are very slow at pH 8 but are greatly facilitated in acidic conditions. The kinetic profiles resemble those of autocatalytic reacting systems, with characteristic induction periods followed by accelerative and leveling phases. Time-dependent CD spectral characteristics indicate the formation of parallel G-tetraplexes before the onset of aggregation. A mechanism for the formation of a novel self-assembled super quadruplex structure of dendrimer-type via interquadruplex $C{\cdot}C^+$ base pairing was speculated on. Recently, however, it was further found that $d(TGG)_4$ can also be induced to form aggregates by molar concentrations of K^+, despite the absence of Ψ-CD formation (Chen, 1997). In fact, it was found that $d(TGG)_4$ is kinetically more facile in forming aggregates than $d(CGG)_4$ at pH 8, suggesting that the presence of cytosine is not essential and is in fact detrimental to aggregation. It was further found that the presence of Mg^{2+} greatly facilitates the aggregate formation and results in the prominent appearance of an intense Ψ-type CD. In an effort to further elucidate the mechanism for the observed self-assembly processes, systematic studies are herein made with oligomers containing XGG trinucleotide repeats, where X = A, C, G, or T, under various chain lengths and ionic conditions.

Received for publication 30 November 1998 and in final form 22 April 1999.

Address reprint requests to Dr. Fu-Ming Chen, Department of Chemistry, Tennessee State University, Nashville, TN 37209-1561. Tel: 615-963-5325; Fax: 615-963-5434; E-mail: chenf@harpo.tnstate.edu.

0006-3495/99/07/410/14 $2.00

Atomic force microscopy (AFM) has been used to characterize structures of various biological macromolecules and their interactions (Hansma and Hoh, 1994). In particular, AFM has recently been used to give direct evidence on the formation of a novel DNA nanostructure termed the *G-wire* (Marsh et al., 1995). Because the proposed mechanisms and structures of the $d(XGG)_4$ aggregates are closely related to those of the G-wire, AFM images of these aggregates will be of considerable interest. This paper reports some of our findings on the kinetic and AFM measurements of these systems. Results indicate that the propensity and morphology of the K^+-induced aggregation of $d(XGG)_n$ depend strongly on the base sequence, the number of repeating units, the nature of terminal bases, and the ionic conditions.

MATERIALS AND METHODS

Synthetic oligonucleotides were purchased from Research Genetics (Huntsville, AL) and used without further purification. These oligomers were purified by the vendor via reverse-phase oligonucleotide purification cartridges and exhibited single-band electrophoretic mobilities in denaturing polyacrylamide gel electrophoresis, with a stated purity of ≥95%. Concentrations of oligomers (per nucleotide) were determined by measuring absorbances at 260 nm after melting, with the use of extinction coefficients obtained via nearest-neighbor approximation, using mono- and dinucleotide values tabulated by Fasman (1975). Aggregation kinetic profiles were obtained by monitoring the time-dependent absorbance changes at 320 nm and maintaining the temperature at 25°C. The reaction was initiated by addition of the appropriate amount of oligomer stock to a buffer solution containing the desired salt concentrations. Thermal denaturation experiments were carried out with 1-cm semimicro cells by monitoring absorbances at appropriate wavelengths. A heating (or cooling) rate of 0.5°C/min was maintained by the temperature controller accessory of a Cary 1E spectrophotometric system. Circular dichroic (CD) spectra were measured with a Jasco J-500A recording spectropolarimeter, using water-jacketed cylindrical cells of 1 cm path length. All experiments were carried out in 10 mM HEPPS (*N*-(2-hydroxyethyl)-piperazine-*N*′-propanesulfonic acid) buffer solutions of pH 8 (adjusted by droplet additions of 1 M NaOH).

DNA solutions (40 μM in nucleotide) used in AFM imaging were those saved from the turbidity kinetic measurements. A volume of 5 μl was deposited on a freshly cleaved mica substrate. The aggregates were allowed to be adsorbed on the surface for ~30 s before being washed with 200 ml of distilled water in a container via rigorous hand agitation for ~20 s and dried overnight in a hood. Imaging was performed in tapping mode with an oxide-sharpened Si_3N_4 tip at room temperature, using a nanoscope III scanning probe microscope with an E-scanner (Digital Instruments). Images were captured under the following conditions: scan rate of 2.6 Hz; drive frequency around 300 kHz; set point ~3 V; an integral-to-proportional gain ratio of 1:10; and 256 scan lines per image.

RESULTS

The nature of the X base strongly affects the propensity of the K^+-induced aggregate formation of oligomers with XGG repeats

The kinetic profiles of aggregate formation via turbidity monitoring at 320 nm for $d(XGG)_4$ in the presence of 2 M KCl are compared in Fig. 1 *A*. It is apparent that $d(GGG)_4$ forms aggregates most readily, whereas $d(CGG)_4$ fails to do so in a time span of 15 h (900 min) at pH 8 and 25°C. The kinetic profiles for $d(AGG)_4$ and $d(TGG)_4$ exhibit autocalalytic-like behaviors, consisting of lag periods or induction times (t_i) of 48 and 45 min, which are followed by accelerative and leveling phases exhibiting characteristic half-times ($t_{1/2}$) of 99 and 118 min, respectively. No apparent lag period ($t_i < 1$ min) appears to be evident for the aggregate formation of $d(GGG)_4$. The 320-nm absorbance decreases at the long-time regions for $d(GGG)_4$ and $d(TGG)_4$ are likely the consequence of slow sedimentation of larger aggregated particulates. These results suggest that the kinetic propensities for the K^+-induced aggregation are strongly sequence dependent and, at pH 8, appear to have the order $d(GGG)_4 > d(TGG)_4 \approx d(AGG)_4 \gg d(CGG)_4$, with $d(TGG)_4$ exhibiting the highest turbidity. It should be noted in passing that 2 M Na^+ failed to induce the observed aggregation phenomenon, and the K^+-induced aggregation of $d(CGG)_4$ is greatly facilitated by a moderate solution acidity (Chen, 1995).

Mg^{2+} greatly facilitates the aggregate formation and acts synergistically with K^+.

Salt concentration-dependent studies led to the finding that the K^+-induced aggregation of $d(XGG)_4$ requires more than 1 M KCl (not shown). Indeed, 1 M KCl failed to induce aggregation of $d(AGG)_4$ and $d(TGG)_4$ in a time span of 15 h. It was found, however, that the presence of Mg^{2+} in the K^+-containing solution can greatly facilitate the aggregation processes. Aggregation kinetic profiles of $d(XGG)_4$ in the presence of 1 M KCl and 16 mM $MgCl_2$ are compared in Fig. 1 *B*. The rates of aggregation are seen to be much faster than those of 2 M KCl and result in much higher turbidity (note the more than twofold scale change in Fig. 1 *B*). Indeed, in the Mg^{2+}-containing solution, a t_i of ~1 min with $t_{1/2}$ of 92 and 31 min were found for $d(AGG)_4$ and $d(TGG)_4$, respectively, and the former exhibits a higher turbidity than the latter, in contrast to their behavior in 2 M KCl. Even $d(CGG)_4$, which exhibits no evidence of aggregation in 2 M KCl, now shows a slow rise in turbidity in the solution containing 1 M KCl and 16 mM $MgCl_2$ with $t_i \approx$ 100 min. The ease of aggregate formation for $d(GGG)_4$ is further manifested by both t_i and $t_{1/2}$ being less than 1 min in the Mg^{2+}-containing solution.

The presence of Mg^{2+} dramatically enhances the thermal stabilities of the aggregates

Fig. 2 *A* compares the thermal melting profiles of aggregates formed with 2 M KCl. The melting temperatures are seen to be ~55°C and do not appear to be strongly sequence dependent. As can be seen in Fig. 2 *B*, the presence of Mg^{2+} greatly enhances the thermal stabilities of the aggregates. The melting temperatures for aggregates of $d(AGG)_4$ and $d(TGG)_4$ in the presence of 1 M KCl and 16 mM $MgCl_2$ are now ~85°C. Interestingly, the turbidity of $d(GGG)_4$ in-

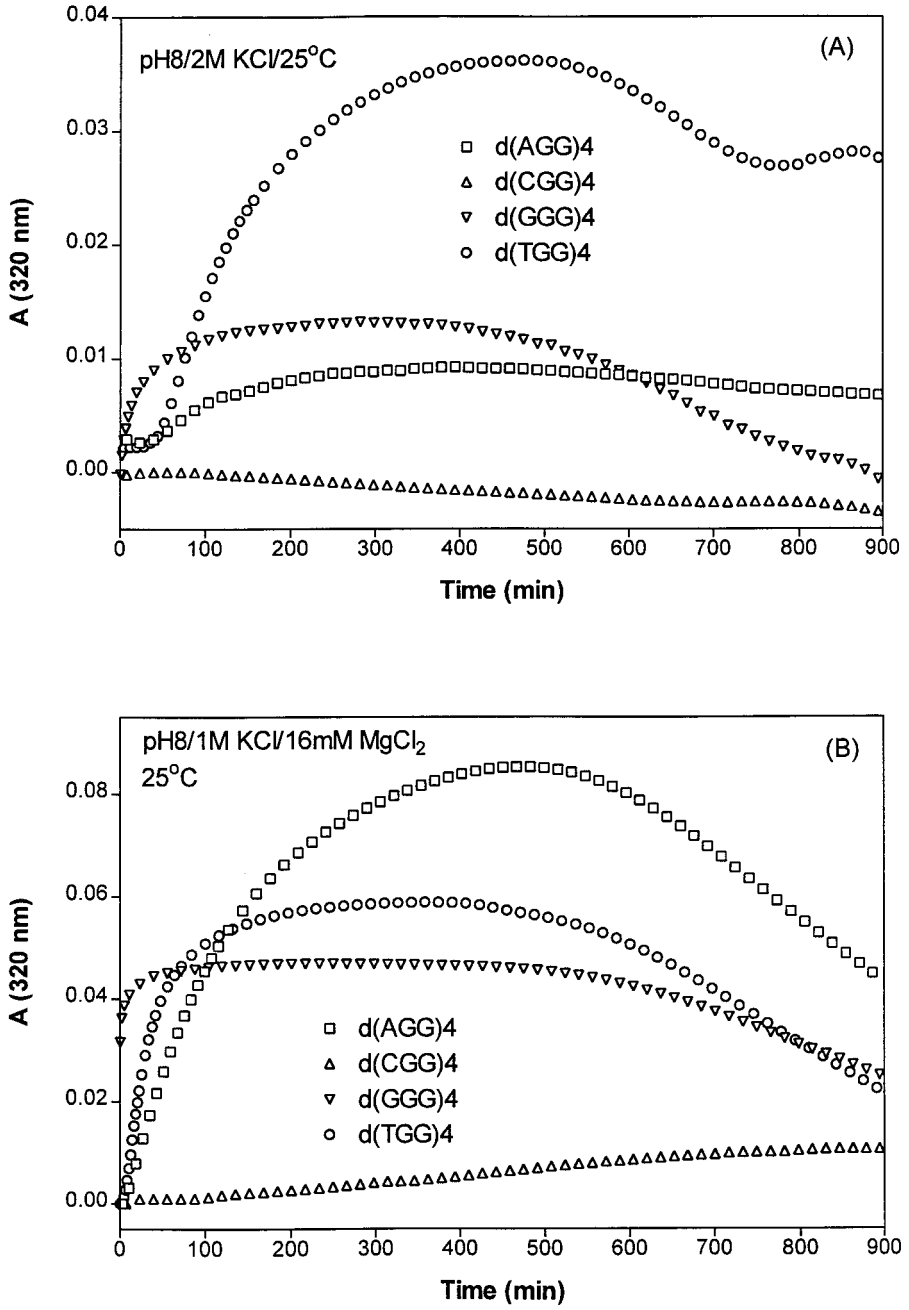

FIGURE 1 Comparison of turbidity-monitored aggregation kinetic profiles at 25°C for 40 μM (in nucleotides) of dodecamers of the form $d(XGG)_4$ in solutions of pH 8 at two different ionic conditions. (*A*) In the presence of 2.0 M KCl. (*B*) In the presence of 1.0 M KCl and 16 mM $MgCl_2$. The solution was first heated to 95°C for 1 min, and the kinetic run started as soon as the solution was cooled back to 25°C. The data have not been corrected for baseline drift or lamp instability because separate experiments with buffer alone at different salt concentrations have indicated a drift of no more than $\pm$0.001 absorbance units at 320 nm in a time span of 900 min.

creases rather than decreases near this same temperature, indicating additional aggregation, and with the disruption of aggregates occurring at temperatures higher than 95°C. Results of the kinetic and melting experiments for $d(XGG)_4$ in the two ionic conditions studied are summarized in Table 1.

Chiroptical properties of the aggregates are strongly sequence dependent, and $d(AGG)_4$ fails to exhibit Ψ-CD characteristics, despite its ease of aggregation

CD spectra of $d(XGG)_4$ in two different solution conditions are compared in Fig. 3. In 2 M KCl solutions (Fig. 3 *A*), only $d(GGG)_4$ exhibits an intense CD spectrum of Ψ-type, with a positive maximum at 260 nm, a shoulder near 285 nm, and a negative tail at longer wavelengths. Despite the significant aggregate formation in 2 M KCl, as indicated by turbidity measurements (see Fig. 1 *A*), $d(TGG)_4$ fails to exhibit Ψ-CD spectral characteristics. In contrast, a huge CD spectrum is induced for $d(TGG)_4$ in the 1 M KCl/16 mM $MgCl_2$ solution, resulting in positive double-hump maxima near 270 and 295 nm and a positive long-wavelength tail (see Fig. 3 *B*). A sizable Ψ-CD was also observed for $d(CGG)_4$ with a maximum at 300 nm, a shoulder near 270 nm, and a positive long-wavelength tail. On the other hand, the CD spectral characteristics of $d(GGG)_4$ are very

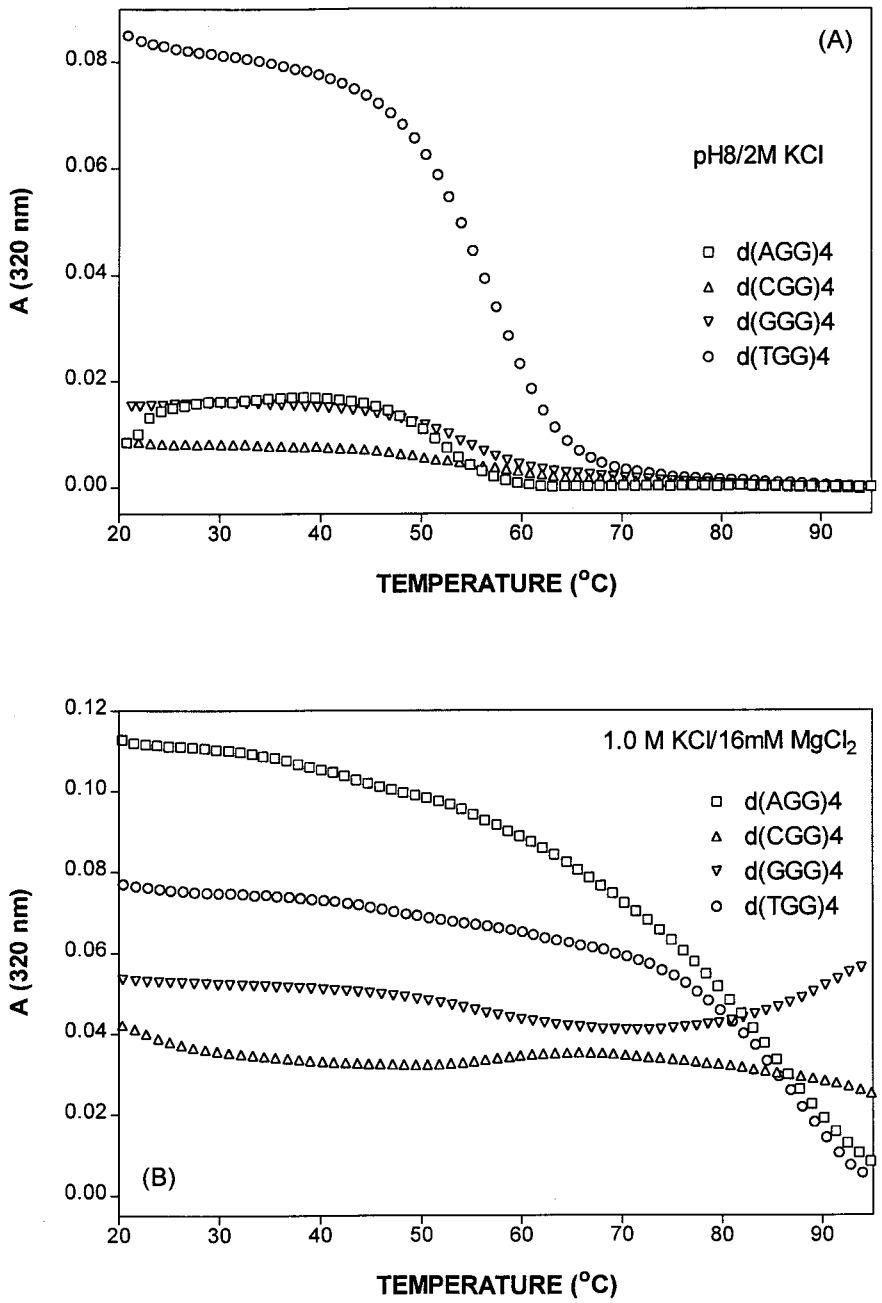

FIGURE 2 Comparison of turbidity-monitored thermal melting profiles of aggregates formed by 40 μM (in nucleotides) of dodecamers of the form $d(XGG)_4$ in solutions of pH 8 at two different ionic conditions. (*A*) In the presence of 2.0 M KCl. (*B*) In the presence of 1.0 M KCl and 16 mM $MgCl_2$. Solutions were allowed to stand for more than 2 days and shaken before the melting run. A heating rate of 0.5°C/min was maintained during the experiment.

similar in the two solutions. It is also of interest to note that $d(AGG)_4$ fails to exhibit Ψ-CD characteristics, despite its considerable aggregate formation in the solution of 1 M KCl/16 mM $MgCl_2$.

The propensity for aggregation is greatly affected by the chain length, with oligomers of four repeating units being most facile

Aggregation kinetic profiles at 20°C for oligomers with three, four, and five trinucleotide repeats are compared in Fig. 4 for oligomers of AGG (*A* and *B*) and TGG (*C* and *D*) repeats at two different solution conditions. In 2 M KCl solutions, the ease of aggregation is seen to follow the order $d(AGG)_4 > d(AGG)_3 \gg d(AGG)_5$ (Fig. 4 *A*). No evidence of aggregate formation is apparent for $d(AGG)_5$ in a time span of 15 h, whereas t_i of 180 and 25 min with $t_{1/2}$ of ~500 and 95 min are found for the three and four repeats, respectively. Again, the facilitation due to the presence of Mg^{2+} is clearly seen in the much faster aggregation kinetics observed in solutions containing 1 M KCl/16 mM $MgCl_2$ (Fig. 4 *B*). Aside from $t_i < 1$ min and $t_{1/2} = 83$ min observed for $d(AGG)_4$, it is interesting to note that in contrast to the absence of aggregation in 2 M KCl solution, $d(AGG)_5$ now exhibits a faster aggregation rate ($t_i = 48$ min, $t_{1/2} = 220$ min) than that of $d(AGG)_3$ ($t_i = 80$ min, $t_{1/2} \approx 500$ min). In contrast, no evidence of aggregation is apparent for both $d(TGG)_3$ and $d(TGG)_5$, whereas $d(TGG)_4$ exhibits aggrega-

TABLE 1 Comparison of kinetic and melting parameters for $d(XGG)_4$ in two different ionic conditions

Oligomer	$[K^+]$ (M)	$[Mg^{2+}]$ (mM)	t_i (min)	ΔA_{max} ($t_{1/2}$, min)	t_m (°C)
$d(AGG)_4$	2		48	0.0093 (99)	53
$d(TGG)_4$	2		45	0.0361 (118)	57
$d(GGG)_4$	2		<1	0.0132 (13)	53
$d(CGG)_4$	2		*		53
$d(AGG)_4$	1	16	1	0.0847 (92)	85
$d(TGG)_4$	1	16	1	0.0589 (31)	87
$d(GGG)_4$	1	16	<1	0.0467 (<1)	>95
$d(CGG)_4$	1	16	~100	[0.0112]	—

Kinetic measurements were made at 25°C, and t_i is the lag time or the induction period before the onset of aggregation. ΔA_{max} is the maximum absorbance change at 320 nm when the kinetic profile becomes asymptotic, and $t_{1/2}$ is the time required for reaching half of this maximum value. Kinetic profiles for which asymptotes were not reached in a time span of 15 h are indicated by brackets, with the absorbance values at 900 min enclosed. The kinetic trace for which no discernible aggregation occurs in a time span of 15 h is designated by *. Thermal denaturation was monitored at 320 nm.

tion in both solution conditions, but with greater facility in the presence of Mg^{2+} (compare Fig. 4, *C* and *D*), having t_i of $<$ 5 versus 60 min and $t_{1/2}$ of 33 versus 209 min, respectively. Results on the effects of chain lengths on the aggregation kinetics are summarized in Table 2.

The nature and the location of the terminal bases strongly affect the aggregation processes

The aggregation kinetic profiles for d(GGXGGXGGXGG) and the related oligomers having X = A or T base attached to one or both end(s) are compared in Fig. 5. It is apparent that in the X = A series (*left panels*), d(GGAGGAGGAGG) is the most facile in forming aggregates in 2 M KCl ($t_i < 1$ min, $t_{1/2} = 17$ min), which is followed by d(AGGAGGAGGAGG) ($t_i = 20$ min, $t_{1/2} = 95$ min), an oligomer with dA added at the 5′ end. Appending dA at the 3′ end or at both terminals results in the absence of turbidity-measurable aggregate formation in 2 M KCl solutions and time spans of 15 h (Fig. 5 *A*). These last two oligomers can, however, readily form aggregates in solutions containing 1 M KCl/16 mM $MgCl_2$, with the oligomer having both ends appended by dA to be most resistant (see Fig. 5 *B*). The ease in aggregation in this ionic condition is shown to follow the order d(GGAGGAGGAGG) ($t_i < 5$ min, $t_{1/2} = 21$ min) > d(AGGAGGAGGAGG) ($t_i < 5$ min, $t_{1/2} = 83$ min) ≈ d(GGAGGAGGAGGA) ($t_i = 10$ min, $t_{1/2} = 55$ min) > d(AGGAGGAGAGGA) ($t_i = 74$ min, $t_{1/2} = 257$ min). For the X = T series, d(GGTGGTGGTGG) and d(TGGTGGTGGTGG) are shown to readily form aggregates, with the former being more facile in 2 M KCl (t_i of <5 versus 60 min and $t_{1/2}$ of 95 versus 209 min), whereas the order appears to be reversed in solutions containing 1 M KCl/16 mM $MgCl_2$ (t_i of 8 versus $<$ 5 min and $t_{1/2}$ of 90 versus 33 min). Neither d(GGTGGTGGTGGT) nor d(TGGTGGTGGTGGT) exhibits aggregation phenomena in a time span of 15 h under both ionic conditions. It thus appears that appending X base at the 3′ end of d(GGXGGXGGXGG) provides a greater hindrance to aggregation than appending X base at the 5′ end. Results on the effects of terminal bases on the aggregation kinetics are summarized in Table 3.

Scanning probe images of aggregates

AFM images of $d(XGG)_4$ aggregates formed in two different solution conditions are compared in Fig. 6. It is immediately apparent that the images of turbidity-measurable aggregates are of sufficient size and can easily be captured by AFM. In the presence of 2 M KCl (*left panels*), $d(GGG)_4$ (Fig. 6 *D*) exhibits the highest density of aggregates formed, which is followed by $d(AGG)_4$ (Fig. 6 *B*) and $d(TGG)_4$ (Fig. 6 *C*), where $d(CGG)_4$ (Fig. 6 *A*) is the lowest. Despite the absence of turbidity at 320 nm (see Fig. 1 *A*), some formation of aggregates is clearly visible for $d(CGG)_4$, albeit smaller in both number and particle size. The particulate size for the $d(TGG)_4$ (Fig. 6 *C*) aggregates appears to be somewhat larger than those of $d(AGG)_4$ (Fig. 6 *B*), despite their similar aggregation densities. This observation is consistent with the significantly higher turbidity exhibited by $d(TGG)_4$ in 2 M KCl (see Fig. 1 *A*). In the presence of $MgCl_2$, the aggregates appear to be considerably elongated (see Fig. 6 *E–H*), in agreement with the much higher turbidities observed (compare Fig. 1, *A* and *B*). The significantly higher aggregate density exhibited by $d(AGG)_4$ than $d(TGG)_4$ (compare Fig. 6, *F* and *G*) appears to be consistent with the higher turbidity observed for the former in this solution (see Fig. 1 *B*). The considerably larger aggregates formed in the presence of $MgCl_2$, in terms of both widths and lengths, are also quite striking for $d(CGG)_4$ (compare Fig. 6, *A* and *E*).

Chain-length-dependent morphologies of aggregates formed in 1 M KCl/16 mM $MgCl_2$ for $d(XGG)_{n = 3–5}$, with X = A (*left panels*) or T (*right panels*), are shown in Fig. 7. As is apparent, the oligomers with four repeats (Fig. 7, *B* and *E*) exhibit the highest aggregation densities, whereas aggregates formed by oligomers with three (Fig. 7, *A* and *D*) and five (Fig. 7, *C* and *F*) repeats are much less numerous. These results are in conformity with those of turbidity measurements indicating the very facile aggregate formation for oligomers with four repeating units (see Fig. 4, *A* and *D*). It should also be noted in passing that the aggregates of $d(TGG)_4$ (Fig. 7 *E*) appear to be significantly elongated when compared with those of $d(AGG)_4$ (Fig. 7 *B*).

AFM images on aggregates formed by oligomers with varying capping bases and in the presence of 1 M KCl/16 mM $MgCl_2$ are shown in Fig. 8. Consistent with the propensities for facile aggregate formation of oligomers with dG at both ends (Fig. 8, *A* and *E*) and dG at the 3′ terminal (Fig. 8, *B* and *F*), high aggregation densities are observed for these oligomers. Except for the somewhat more elongated features for the T-containing oligomers, no great

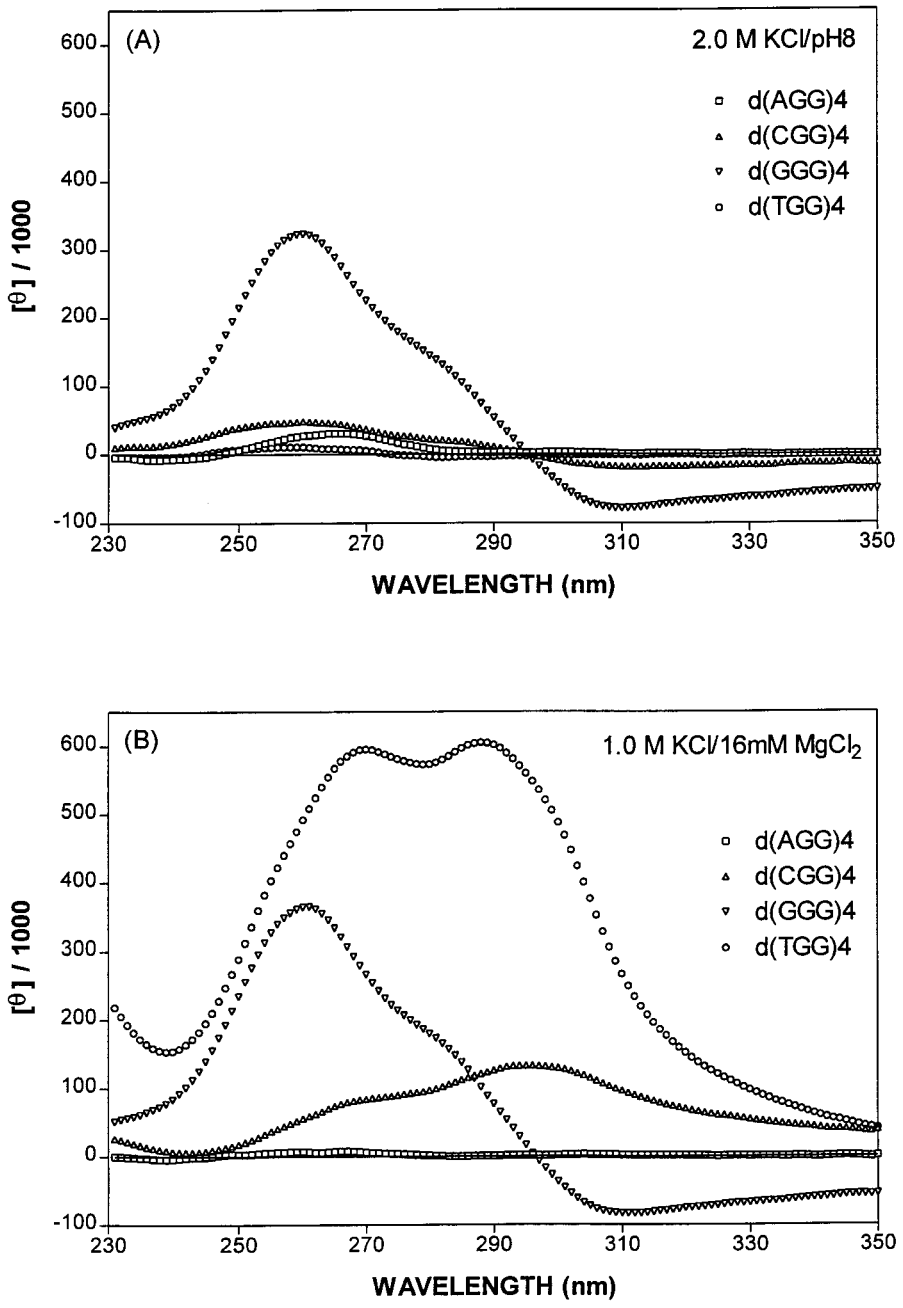

FIGURE 3 Comparison of CD spectral characteristics at room temperature for 40 μM of dodecamers of the form $d(XGG)_4$ in solutions of pH 8 at two different ionic conditions. (*A*) In the presence of 2.0 M KCl. (*B*) In the presence of 1.0 M KCl and 16 mM $MgCl_2$. Solutions were heated to 95°C and cooled back to room temperature (with a 10-day wait) before the CD measurements.

difference in aggregation density is found among them. On the other hand, oligomers capped with dA or dT at the 3′ end (Fig. 8, *C* and *G*) exhibit shorter aggregates and much lower aggregation density, whereas those with both ends capped exhibit sparsely formed aggregates (Fig. 8, *D* and *H*). The much greater hindrance of aggregate formation with a dA or dT capped at the 3′ end than with a dA or dT capped at the 5′ end is dramatically illustrated via comparison of Fig. 8, *B* or *F*, versus Fig. 8, *C* or *G*, respectively.

Kinetics of aggregate formation were also investigated by AFM, by taking images of the d(GGAGGAGGAGG) aggregating solution at various times. Progressive increase in the density of aggregates is clearly visible for images taken 1, 2, 4, and 8 h after the 2 M KCl addition (results not shown).

DISCUSSION

Systematic aggregation studies with various oligomers of XGG trinucleotide repeats under different ionic conditions led to the following findings: 1) More than 1 M KCl is needed to observe the turbidity-measurable aggregation for these oligomers (40 μM in nucleotide and at 25°C), and NaCl fails to induce a similar phenomenon. 2) Acting synergistically with K^+, the presence of Mg^{2+} greatly facilitates the aggregate formation and dramatically enhances the

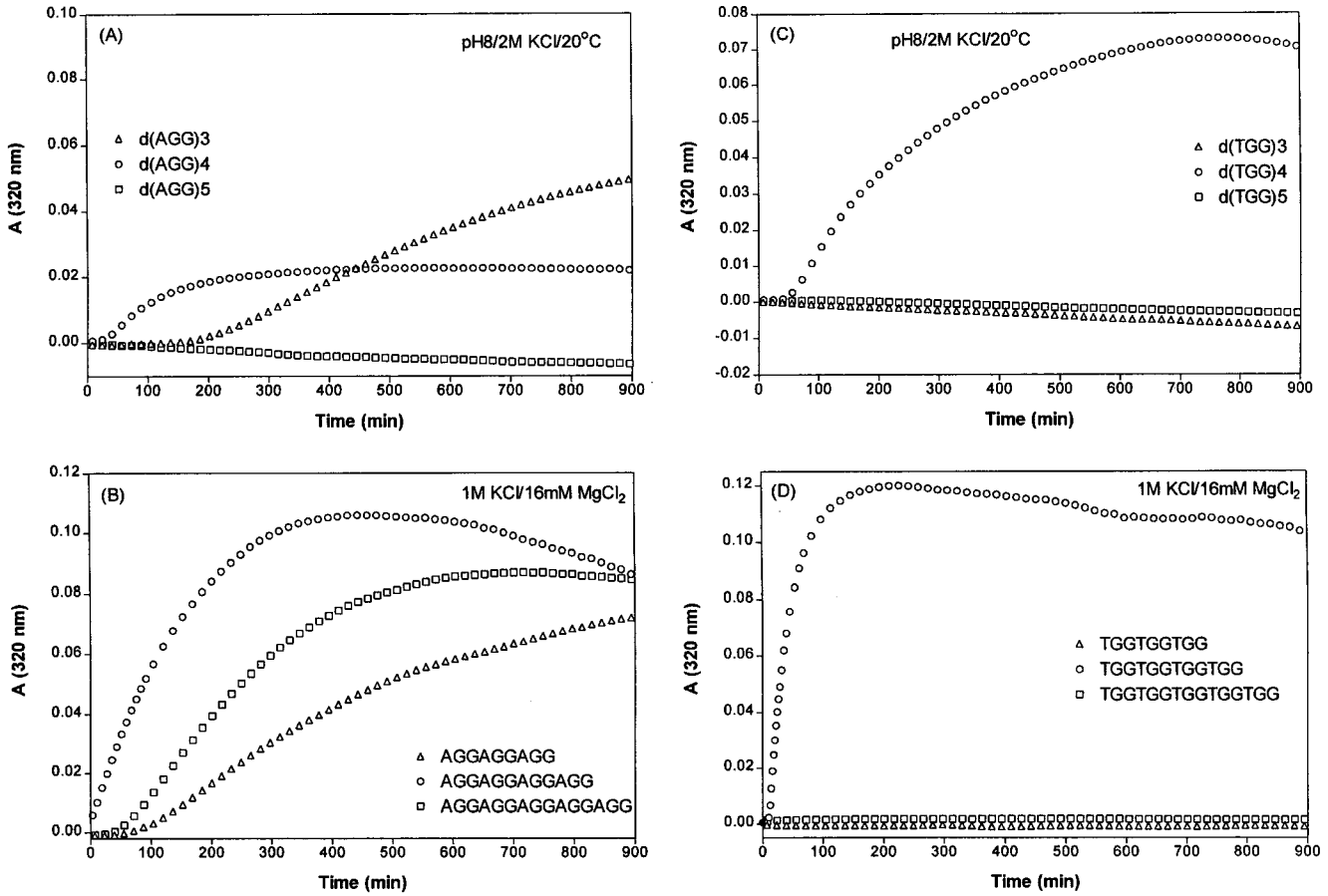

FIGURE 4 Comparison of aggregation kinetic profiles at 20°C of 40 μM $d(AGG)_n$ and $d(TGG)_n$ in solutions of pH 8 at two different ionic conditions. (*A*) $d(AGG)_n$ in the presence of 2.0 M KCl. (*B*) $d(AGG)_n$ in the presence of 1.0 M KCl and 16 mM $MgCl_2$. (*C*) $d(TGG)_n$ in the presence of 2.0 M KCl. (*D*) $d(TGG)_n$ in the presence of 1.0 M KCl and 16 mM $MgCl_2$.

thermal stabilities of the aggregates formed. 3) The nature of the X base strongly affects the propensity of the K^+-induced aggregate formation, and at pH 8 the observed order appears to be $d(GGG)_4 > d(AGG)_4 \approx d(TGG)_4 \gg$ $d(CGG)_4$, with CGG repeats greatly facilitated by moderate acidities. 4) Chiroptical properties of the aggregates depend strongly on the base sequence and ionic conditions of the solution, e.g., $d(TGG)_4$ exhibits intense Ψ-CD characteristics, distinct from those of $d(GGG)_4$, in the presence but not in the absence of Mg^{2+}, whereas despite its relative ease of aggregate formation, $d(AGG)_4$ fails to exhibit Ψ-CD characteristics, even in the presence of Mg^{2+}. 5) The propensity for aggregation is greatly affected by the chain length, with oligomers of four repeats being most facile. 6) The nature and location of the terminal bases also strongly affect the aggregation processes; appending with X = A or T base at the 3′ end of d(GGXGGXGGXGG) appears to provide a greater hindrance to aggregation than appending an X base at the 5′ end. 7) Both $d(AAGG)_4$ and $d(TTGG)_4$ failed to exhibit the K^+-induced aggregation phenomena, even in the presence of Mg^{2+} (results not shown).

TABLE 2 Effects of chain lengths on the aggregation kinetics at 20°C

Oligomer	$[K^+]$ (M)	$[Mg^{2+}]$ (mM)	t_i (min)	ΔA_{max} ($t_{1/2}$, min)
AGGAGGAGG	2		180	[0.0494] (~500)
AGGAGGAGGAGG	2		25	0.0225 (95)
AGGAGGAGGAGGAGG	2		*	
TGGTGGTGG	2		*	
TGGTGGTGGTGG	2		60	0.0729 (209)
TGGTGGTGGTGGTGG	2		*	
AGGAGGAGG	1	16	80	[0.0761]
AGGAGGAGGAGG	1	16	<1	0.1053 (83)
AGGAGGAGGAGGAGG	1	16	48	0.0870 (220)
TGGTGGTGG	1	16	*	
TGGTGGTGGTGG	1	16	<5	0.1196 (33)
TGGTGGTGGTGGTGG	1	16	*	

*See Table 1 footnote.

A speculative model was earlier proposed by us (Chen, 1997) to rationalize the self-assembly phenomenon of $d(TGG)_4$. This same mechanism may also be operative in oligomers with XGG trinucleotide repeats in general. The oligomer likely first forms parallel-stranded homoduplexes in the K^+-containing solutions, which in turn form in-

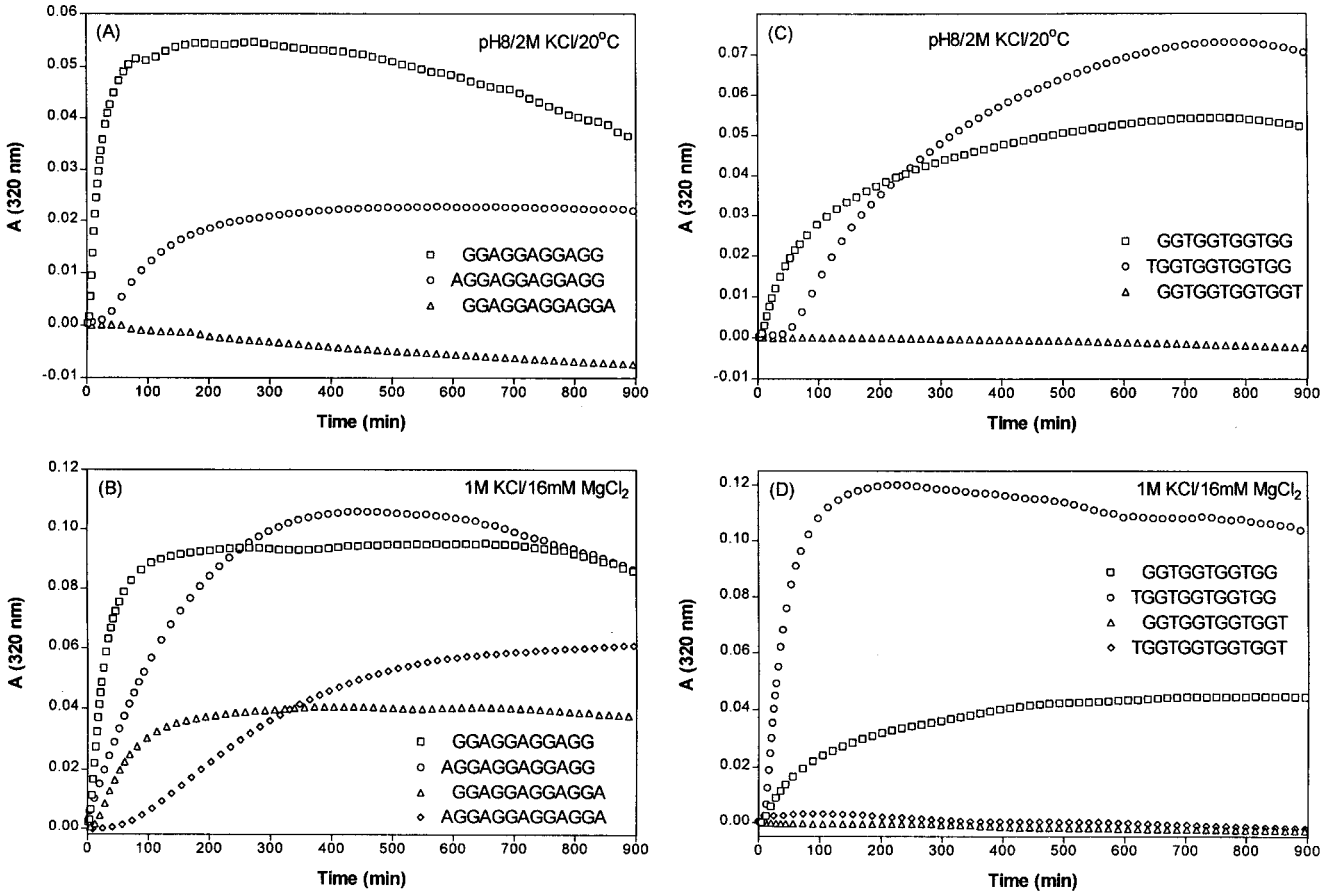

FIGURE 5 Comparison of aggregation kinetic profiles at 20°C of 40 μM d(GGXGGXGGXGG) and related oligomers in solutions of pH 8 at two different ionic conditions. (*A*) X = A in the presence of 2.0 M KCl. (*B*) X = A in the presence of 1.0 M KCl and 16 mM $MgCl_2$. (*C*) X = T in the presence of 2.0 M KCl. (*D*) X = T in the presence of 1.0 M KCl and 16 mM $MgCl_2$. Kinetic profiles for d(XGGXGGXGGXGGX) are nearly identical to those of d(GGXGGXGGXGGX) in *A* and *C* and are not shown.

and/or out-of-registered quadruplexes (presumably aided by the optimal size of K^+ that fits into quadruplex cages). Axial extension of the out-of-register quadruplexes could result if repeated quadruplex formation occurred with sticky ends to form G-wires (Marsh and Henderson, 1994), whereas those of in-register quadruplexes could result from head-to-tail stacking. In addition, lateral expansion could be achieved by interquadruplex association via phosphate-Mg^{2+} bond formation.

The need for molar concentration of KCl to form turbidity-measurable aggregation and the inability of Na^+ to do likewise may be a consequence of their differential effectiveness in inducing parallel quadruplex formation. Raman studies by Miura et al. (1995) on the quadruplex formation of $d(TTTTGGGG)_4$ led to the finding that both Na^+ and K^+ facilitate an antiparallel foldback quadruplex at low salt concentrations but a parallel quadruplex at higher concentrations, with K^+ being more effective in inducing the parallel association. It has long been suggested that the greater thermal stability of DNA quadruplex structures in the presence of K^+ is primarily a result of the optimal fit of this ion in the coordination sites formed by G quartets. However, Hud et al. (1996) have recently argued that such a preference is actually driven by the greater energetic cost of Na^+ dehydration with respect to K^+ dehydration.

The observed synergistic effects of K^+ and Mg^{2+} may be the consequence of complementary roles played by these two cations—the ability to facilitate the parallel quadruplex formation of the former and binding to phosphates by the latter. The inability of Mg^{2+} to induce aggregation in the absence of K^+ supports the important role of parallel quadruplex formation in the supramolecular self-assembly in $d(XGG)_4$. In view of its strong affinity for phosphates, the role of Mg^{2+} in the self-assembly process may be twofold: 1) facilitation of the initial homoduplex and subsequent tetraplex formation for axial extension via phosphate charge neutralization and 2) bridging interquadruplex phosphate groups for lateral expansion.

The speculated mechanism appears to be consistent with the finding that $d(GGG)_4$ is more facile than $d(AGG)_4$ and $d(TGG)_4$ in aggregate formation, which in turn aggregate more readily than $d(CGG)_4$ at pH 8, with the aggregation of C-containing oligomer being facilitated by acidic conditions. The ability to form out-of-register quadruplexes with-

TABLE 3 Effects of terminal bases on the aggregation kinetics at 20°C

Oligomer	$[K^+]$ (M)	$[Mg^{2+}]$ (mM)	t_i (min)	ΔA_{max} ($t_{1/2}$, min)
GGAGGAGGAGG	2		<1	0.0576 (17)
AGGAGGAGGAGG	2		20	0.0225 (95)
GGAGGAGGAGGA	2	*		
GGTGGTGGTGG	2		<5	0.0542 (95)
TGGTGGTGGTGG	2		60	0.0729 (209)
GGTGGTGGTGGT	2		*	
GGAGGAGGAGG	1	16	<5	0.0928 (21)
AGGAGGAGGAGG	1	16	<5	0.1033 (83)
GGAGGAGGAGGA	1	16	10	0.0405 (55)
AGGAGGAGGAGGA	1	16	74	0.0520 (257)
GGTGGTGGTGG	1	16	8	0.0443 (90)
TGGTGGTGGTGG	1	16	<5	0.1196 (33)
GGTGGTGGTGGT	1	16	*	
TGGTGGTGGTGGT	1	16	*	

*See Table 1 footnote.

out the constraints of the intervening non-G bases likely accounts for its ease of aggregation for $d(GGG)_4$. On the other hand, the presence of cytosines in $d(CGG)_4$ may have trapped this oligomer in conformations that utilize G·C base pairings at pH 8, such as dimeric duplexes or monomeric hairpins, so as to hinder quadruplex formation. Thus the acid-facilitated aggregation of $d(CGG)_4$ may partly be the consequence of the destabilization of these trapped conformers resulting from weakened G·C base pairs due to base protonation of the cytidine, and partly the consequence of the facilitation of parallel duplex and/or quadruplex formation via $C{\cdot}C^+$ base pairing (Chen, 1995).

The inability of $d(AAGG)_4$ and $d(TTGG)_4$ to form aggregates is most likely the consequence of constraints and steric hindrance introduced by intervening and two terminal non-G bases in forming appropriate G-quadruplexes for axial extension. Similarly, the effect of capping oligomers with non-G bases on aggregation may be attributed to the steric hindrance of quadruplex formation due to the presence of these bases. Thus it is understandable that capping both ends will provide a greater resistance to aggregate formation than a single cap at either end of the oligomer. It is less clear, however, why capping at the 3′ end will render a considerably greater hindrance of aggregation than capping at the 5′ end. The chain length dependence may partly be rationalized in terms of hairpin formation. The oligomer with five repeats may be long enough to be easily trapped into hairpin conformations to become less efficient in parallel quadruplex formation than the ones with three or four repeating units, where the latter are more facile because of the larger numbers of G-quartet formed.

It is noteworthy that the appearance of Ψ-CD spectral characteristics is related to the chirality and other characteristics of the formed superstructure. It is well known that the CD spectrum of an optically active molecule can sometimes change drastically when the molecule becomes part of a larger aggregate particle (Tinoco et al., 1980). When this aggregate reaches a size comparable to the wavelength of the light used in the CD experiment, anomalous spectral changes occur. A long tail often apppears in the CD at wavelengths outside the absorption bands of the constituent molecules, and as the aggregate particles grow in size, the magnitudes and band shapes of the CD inside the absorption bands also change. The origin of the tail anomalies has been attributed to the ability of large chiral particles to preferentially scatter right or left circularly polarized light away from the transmitted beam (Bustamante et al., 1983). On the other hand, the physical origin of the nonscattering Ψ-type CD anomalies is that when the dimensions of a chiral object are similar to the wavelength of the incident light, the large-scale handedness of the object will have a much greater effect in enhancing or suppressing the absorption of circularly polarized light than when the chiral object is small compared to wavelength. In large, dense chiral molecular aggregates, the eigenmodes of excitation are greatly delocalized throughout the entire aggregate particle, which necessitates the inclusion of intermediate and radiation coupling mechanisms in addition to the static dipole coupling (Keller and Bustamante, 1986). It was found that long-range coupling is possible when the aggregate is three-dimensional and large (~1/4 λ) and has a high density of chromophores. Deficiency in one or more of these factors likely accounts for the absence of Ψ-CD in some of our sequences and other G-rich polymers observed in other laboratories under lower salt concentrations.

Superstructures formed by G-rich DNAs have been observed previously in the presence of K^+ by others, although in ionic strengths of no more than 1 M. Sen and Gilbert (1992) reported that oligomers with a single multiguanine (more than 3 Gs) motif at their 3′ or 5′ end can form higher order products, consisting of 8, 12, and 16 strands. Based on their methylation protection experiments, a nested head-to-tail superstructure containing two or more tetraplexes bonded front to back via G quartet formation of out-of-registered guanines was suggested. It was noted that superstructural formation was achieved in a buffer containing KCl but not in a buffer containing NaCl. It was further shown by Lu et al. (1992) that in the presence of K^+, but not Na^+, higher order complexes are formed in dT_4G_4. The presence of a T at the 3′ end inhibits such association in dT_4G_4T. Formation of these superstructures usually requires high salt as well as high oligonucleotide concentrations, and the limited number of superstructures formed may have resulted from steric hindrance caused by the protruding T-tails.

Marsh and Henderson (1994) later found that the telomeric DNA oligonucleotide 5′-GGGGTTGGGG-3′ spontaneously assembles into large superstructures (*termed G-wires*) that can be resolved by gel electrophoresis as a ladder pattern, most efficiently in Na^+, but a greater degree of stability was acquired by the addition of K^+. Its self-association is noncovalent and exhibits characterstics of

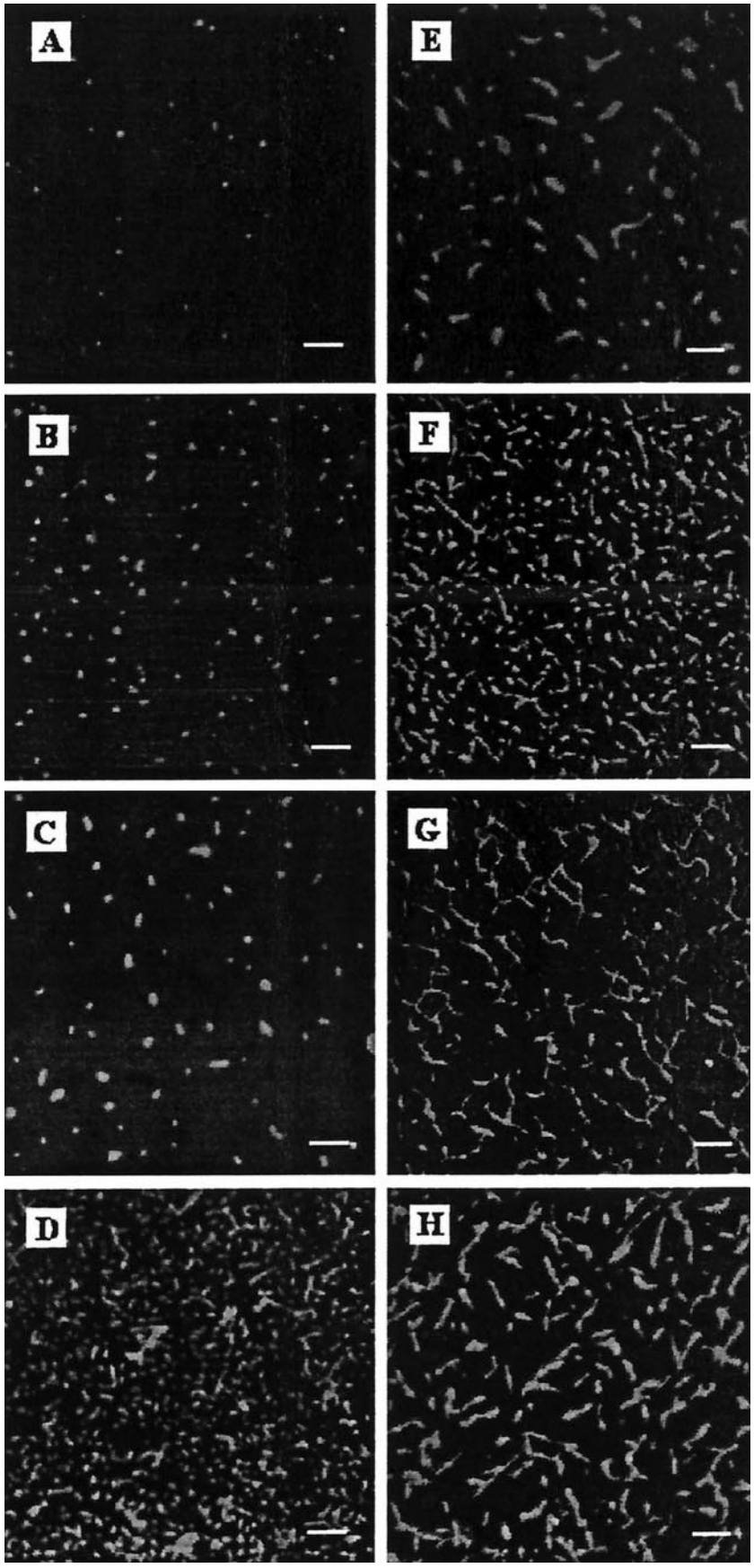

FIGURE 6 Comparison of AFM images of aggregates formed by $d(XGG)_4$ in two different ionic conditions: 2 M KCl (*left panels*) and 1 M KCl/16 mM $MgCl_2$ (*right panels*). (*A* and *E*) $d(CGG)_4$; (*B* and *F*) $d(AGG)_4$; (*C* and *G*) $d(TGG)_4$; (*D* and *H*) $d(GGG)_4$. All scale bars are 150 nm.

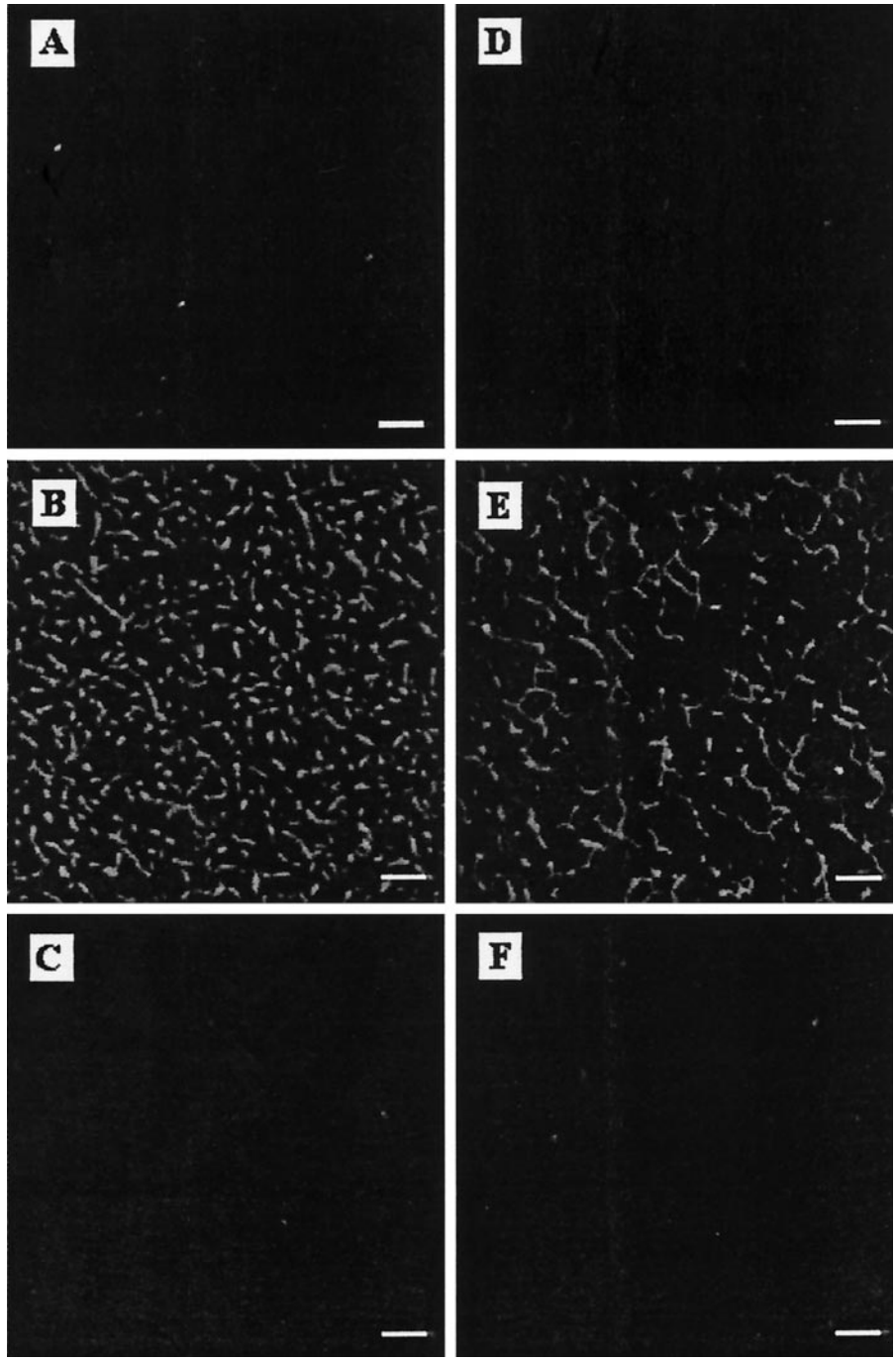

FIGURE 7 Effects of chain length on the AFM images of aggregates formed in solutions containing 1 M KCl/16 mM $MgCl_2$. (*A*) $d(AGG)_3$; (*B*) $d(AGG)_4$; (*C*) $d(AGG)_5$; (*D*) $d(TGG)_3$; (*E*) $d(TGG)_4$; (*F*) $d(TGG)_5$. All scale bars are 150 nm.

G4-DNA, a parallel four-stranded structure stabilized by guanine tetrads. The spontaneous self-assembly into large polymers is likely facilitated by the presence of blocks of guanines at both the 5′ and 3′ ends. It was proposed that the G-wire consists of G4-DNA domains punctuated by T nodes. The initial starting structure consists of a G4 domain containing four quartets formed by the association of the 5′ half of a duplex with the 3′ half of another duplex, forming a slipped tetraplex structure with G-duplex "sticky ends." The strands run parallel to each other and can accept an additional duplex at either end, reminescent of the slipped architecture proposed by Sen and Gilbert (1992) for their observed superstructures.

Subsequently, the morphology of G-wires was investigated by AFM (Marsh et al., 1995). The length of G-wires was found to range from 10 to >1000 nm, and the height and width of G-wires appeared to be uniform, with few bends, kinks, or branches. This indicated that G-wires were ordered, relatively rigid polymers. Magnesium induced synergy of G-wire self-assembly. The height of G-wires was found to be two to three times greater than the height of plasmid DNA in the AFM, ranging from 12.7 to 23.9 Å,

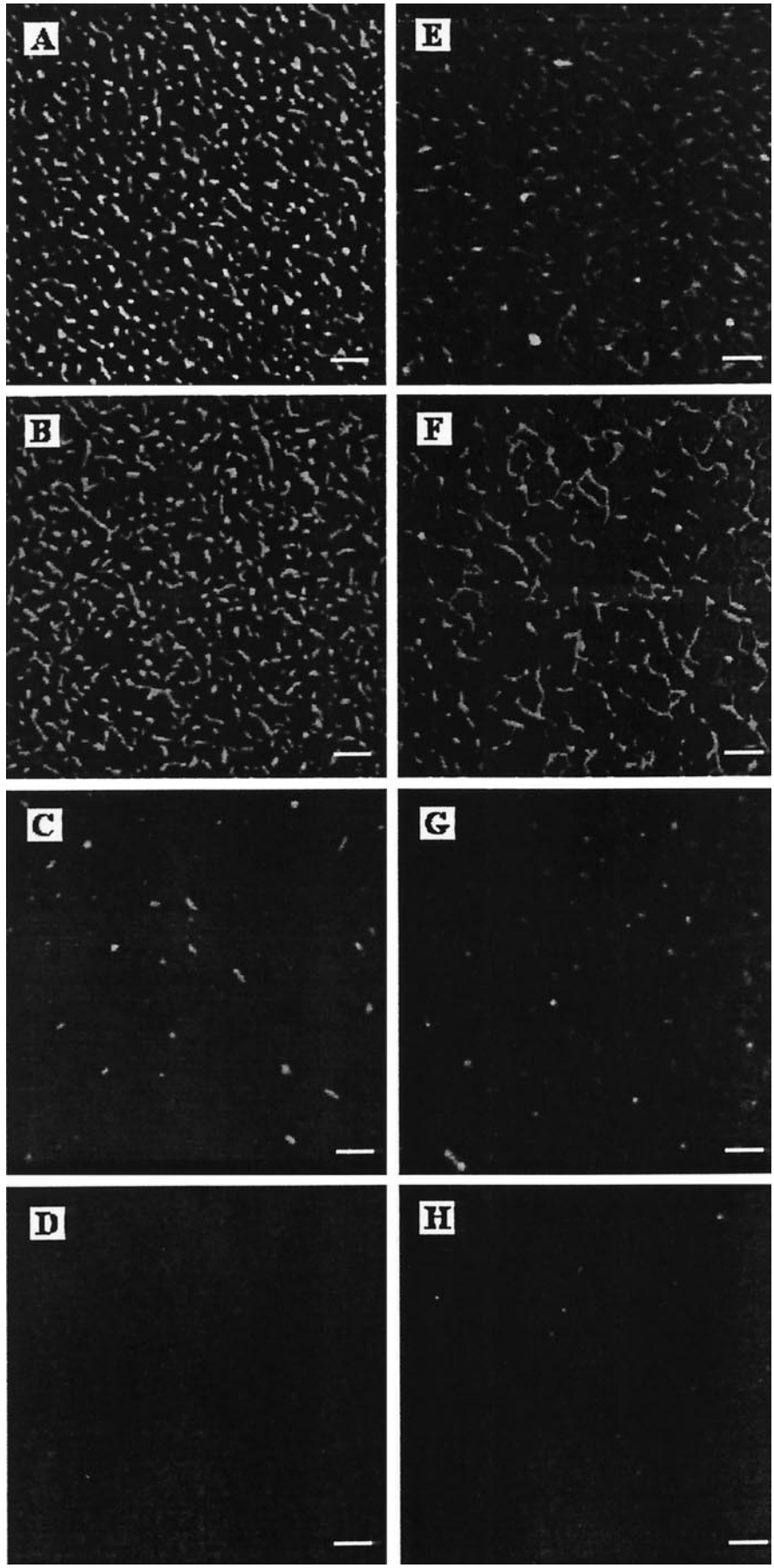

FIGURE 8 Comparison of AFM images of aggregates formed by oligomers with differing terminal base in solutions containing 1 M KCl/16 mM $MgCl_2$. (*A*) d(GGAGGAGGAGG); (*B*) d(AGGAGGAGGAGG); (*C*) d(GGAGGAGGAGGA); (*D*) d(AGGAGGAGGAGGA); (*E*) d(GGTGGTGGTGG); (*F*) d(TGGTGGTGGTGG); (*G*) d(GGTGGTGGTGGT); (*H*) d(TGGTGGTGGTGGT). All scale bars are 150 nm.

depending on the ionic conditions. The height of G-wires measured in the AFM under some conditions was close to the diameter of G-quartets determined by x-ray crystallography (~28 Å) (Kang et al., 1992; Laughlan et al., 1994). Interestingly, assembly of G-wires occurred most efficiently in Na^+, yet a greater degree of stability was acquired by the addition of K^+. This is at odds with our observation that Na^+ is ineffective in inducing the aggregation phenomenon in the XGG trinucleotide repeats.

A related structure was later reported by Dai et al. (1995) for the $C_4T_4G_4T_{1-4}G_4$ series of oligomers, which self-assemble into multistranded species of high molecular weight in the presence of 100 mM K^+ plus 20 mM Mg^{2+}. Data suggest that these higher order species arise from successive additions of parent oligomer to an initially formed quadruplex. Because the self-assembly is not observed with K^+ or Mg^{2+} alone, these cations behave in a synergistic manner in the formation and/or stability of the supermolecular self-assemblies. Subsequently, Marotta et al. (1996) studied DNA oligomers possessing $G_xT_2G_y$ segments. Electrophoresis of these oligomers in the presence of both 100 mM K^+ and 20 mM Mg^{2+} gives a ladder of multiple bands of high molecular weight, indicative of multistranded DNA formation. The results indicate that self-assembly into high-molecular-weight species is favored by the presence of Mg^{2+} as well as the presence of four or more bases in the terminal G_y segment.

In addition to the duplex and quadruplex formation in d(GGGGCCCC), Deng and Braunlin (1995) noted the broadening of proton resonances and the appearance of a series of slower moving faint gel electrophoretic bands in their titration studies with KCl, indicating the formation of some higher order structures in the presence of added KCl. Furthermore, Protozanova and Macgregor (1996) found that in aqeous solutions containing mono- and divalent cations, the oligomer $d(A_{15}G_{15})$ readily self-assembles into high-molecular-weight species that resolve as discrete bands on native and denaturing electrophoresis gels. In the proposed model for the oligomers and polymers of $d(A_{15}G_{15})$, several molecules of the monomers interact via a stem of tetraplex structure formed by the guanine residues. The 5′ end adenine forms single-stranded arms that are displaced from the guanine-containing stem. In deference to the G-wires introduced by Marsh and Henderson (1994), these structures were called *frayed wires*. Divalent cations at millimolar concentrations lead to the formation of the polymers, whereas the presence of the monovalent cations stabilizes lower-molecular-weight complexes consisting of two to six strands of $d(A_{15}G_{15})$. The data showed that stable frayed wires form only when there are between four and eight guanosine residues at the 3′ end of the oligomer.

All of these observations are likely related to the self-aggregation phenomena observed in our XGG trinucleotide repeating systems. As for the possible biological significance of these observations, it is interesting to note that the single-stranded termini of all chromosomal telomeres sequenced to date have a guanine motif at their 3′ termini, with guanine as the terminal base. Given a sufficient local density of telomeres in the potassium-rich environment of the cell with some presence of Mg^{2+}, these higher order superstructures may arise. This suggests that the structure of telomeric DNA may be quite unusual. Although the salt concentrations of 2 M KCl and 1 M KCl/16 mM KCl employed in this report are far from being physiological conditions, it should be noted that the onsets of aggregation in a time frame of less than 15 h have been observed in solutions containing only mM concentrations of K^+ and Mg^{2+}. Examples are $d(TGG)_4$ in the presence of 2 mM KCl/16 mM $MgCl_2$ (Chen, 1997), $d(AGG)_4$ in the presence of 40 mM KCl/16 mM $MgCl_2$, and d(GGAGGAGGAGG) and d(GGTGGTGGTGG) in the presence of 16 mM KCl/16 mM $MgCl_2$ (not shown).

We thank Dr. Yei-ShinTung for his help during the course of AFM measurements.

This work was supported by Army Medical Research grant DAMD17-94-J-4474 and a subproject of Minority Biomedical Research Support (MBRS) grant S06GM0892.

REFERENCES

Blackburn, E. H. 1994. Telomeres: no end in sight. *Cell.* 77:621–623.

Bustamante, C., I. Tinoco, Jr., and M. F. Maestre. 1983. Circular differential scattering can be an important part of the circular dichroism of macromolecules. *Proc. Natl. Acad. Sci. USA.* 80:3568–3572.

Chen, F.-M. 1995. Acid-facilitated supramolecular assembly of G-quadruplexes in $d(CGG)_4$. *J. Biol. Chem.* 270:23090–23096.

Chen, F.-M. 1997. Supramolecular self-assembly of $d(TGG)_4$, synergistic effects of K^+ and Mg^{2+}. *Biophys. J.* 73:348–356.

Dai, T.-Y., S. P. Marotta, and R. D. Sheardy. 1995. Self-assembly of DNA oligomers into high molecular weight species. *Biochemistry.* 34: 3655–3662.

Deng, H., and W. H. Braunlin. 1995. Duplex to quadruplex equilibrium of the self-complementary oligonucleotide d(GGGGCCCC). *Biopolymers.* 35:677–681.

Fasman, G. D., editor. 1975. CRC Handbook of Biochemistry and Molecular Biology: Nucleic Acids, Vol. 1, 3rd Ed. CRC Press, Cleveland, OH. 589.

Hansma, H. G., and H. Hoh. 1994. Biomolecular imaging with the atomic force microscope. *Annu. Rev. Biophys. Biomol. Struct.* 23:115–139.

Hud, N. V., F. W. Smith, F. A. L. Anet, and J. Feigon. 1996. The selectivity for K^+ versus Na^+ in DNA quadruplexes is dominated by relative free energies of hydration: a thermodynamic analysis by ^1H NMR. *Biochemistry.* 35:15383–15390.

Kang, C. H., X. Zhang, R. Ratliff, R. Moyzis, and A. Rich. 1992. Crystal structure of four-stranded Oxytricha telomeric DNA. *Nature.* 356: 126–131.

Keller, D., and C. Bustamante. 1986. Theory of the interaction of light with large inhomogeneous molecular aggregates. II. Psi-type circular dichroism. *J. Chem. Phys.* 84:2972–2980.

Laughlan, G., A. I. H. Murchie, D. G. Norman, M. H. Moore, P. C. E. Moody, D. M. Lilley, and B. Luisi. 1994. The high resolultion crystal structure of a parallel-stranded guanine tetraplex. *Science.* 265:520–524.

Lu, M., Q. Guo, and N. R. Kallenbach. 1992. Structure and stability of sodium and potassium complexes of dT_4G_4T. *Biochemistry.* 31: 2455–2459.

Lu, M., Q. Guo, and N. R. Kallenbach. 1993. Thermodynamics of G-tetraplex formation by telomeric DNAs. *Biochemistry.* 32:598–601.

Lumdblad, L. L., and J. W. Szostak. 1989. A mutant with a defect in telomere elongation leads to senescence in yeast. *Cell.* 57:633–643.

Marotta, S. P., P. A. Tamburri, and R. D. Sheardy. 1996. Sequence and environmental effects on the self-assembly of DNA oligomers possessing $G_xT_2G_y$ segments. *Biochemistry.* 35:10484–10492.

Marsh, T. C., and E. Henderson. 1994. G-wires: self-assembly of a telomeric oligonucleotide, d(GGGGTTGGGG), into large superstructures. *Biochemistry.* 33:10718–10724.

Marsh, T. C., J. Vesenka, and E. Henderson. 1995. A new DNA nanostructure, the G-wire, imaged by scanning probe microscopy. *Nucleic Acids Res.* 23:696–700.

Miura, T., J. M. Benevides, and G. J. Thomas, Jr. 1995. A phase diagram for sodium and potassium ion control of polymorphism in telomeric DNA. *J. Mol. Biol.* 248:233–238.

Protozanova, E., and R. B. Macgregor, Jr. 1996. Frayed wires: a thermally stable form of DNA with two distinct structural domains. *Biochemistry.* 35:16638–16645.

Sandell, L. L., and V. A. Zakian. 1993. Loss of a yeast telomere: arrest, recovery, and chromosome loss. *Cell.* 75:729–739.

Sen, D., and W. Gilbert. 1988. Formation of parallel four-stranded complexes by guanine-rich motifs in DNA and its implications for meiosis. *Nature.* 334:364–366.

Sen, D., and W. Gilbert. 1992. Novel DNA superstructures formed by telomere-like oligomers. *Biochemistry.* 31:65–70.

Tinoco, I., C. Bustamante, and M. F. Maestre. 1980. The optical activity of nucleic acids and their aggregates. *Annu. Rev. Biophys. Bioeng.* 9:107–141.

Williamson, J. R. 1994. G-quartet structures in telomeric DNA. *Annu. Rev. Biophys. Biomol. Struct.* 23:703–730.